TESTS ON BEAM TO CFT-RHS COLUMN CONNECTIONS APPLYING SLIP-CRITICAL BLIND BOLTS

WEIFENG JIAO[1], YIYI CHEN[1] and WEI WANG[1]

[1]*State Key Laboratory of Disaster Reduction in Civil Engineering, Tongji University, Shanghai, China.*
E-mail: jiaoweifeng@163.com
yiyichen@tongji.edu.cn
weiwang@tongji.edu.cn

A slip-critical blind bolt (SCBB) technique has been developed for the connection of tubular members. Recently with an improvement of the SCBB by additive sleeve infilling the enlarged bolt holes, the tests of beam to concrete filled tube-rectangular hollow section (CFT-RHS) column joint were designed and carried out to investigate the seismic behaviors. The basic configuration of the joint was the planar cruciform with stiffened extended end-plate of beam connected through SCBB to the columns, while the CFT-RHS steel tube wall was with moderate thickness and no additional stiffeners existed. The design of the specimens followed the criteria of strong column-weak beam. Three types of specimens were constituted: one with the uniform built-up section beam, the second with reduced section beam (dog-bone section), and the third one with concrete slab over the beam. The beam tip loads were cyclically applied with the increasing displacements. The tests show that the joint functions during the whole loading process till to the storey drift larger than 0.04 to 0.06; full flexural stiffness and moment capacity can be realized; and no slippage of the contact surface between column wall and end-plate occurs. This study reaches the conclusions that SCBB with additive sleeves could meet the seismic requirements to the beam-column joint for moment resistant frames.

Keywords: beam-column joint; CFT tubular column; slip-critical blind bolts; cyclic loading tests.

1 Introduction

In recent years, blind bolts have been applied to the joints between rectangular hollow section (RHS) tubes as well as RHS tube and open section member. These kinds of bolts overcome the problem to tighten the high strength bolts inside of the tube.

Nowadays, Hollo-bolts developed by Lindapter International Company in Britain are paid more attention. The assembly of Hollo-bolt consists of five parts: bolt shank, collar, rubber washer, flaring sleeve and thread cone (Tizani 2003, Xu 2015). Bolted joints with hollo-bolts can generally be divided into three types, including end-plate joint (Wang 2010), T-stub joint (Loh 2006, Wang 2009, Wang 2013) and angle joint (Elghazouli 2009, Liu 2012). Nonetheless, Xu (2015) investigated the mechanical properties of Hollo-bolts and discovered that the pre-tension force of Hollo-bolt under design torque could not meet the requirement of pre-tightening mechanism in Chinese code (2017). The failure mode of Hollo-bolt under shear force was the damage of sleeve and its failure load was much less than that of bolt shank.

Proceedings of the 17th International Symposium on Tubular Structures.
Editors: X.D. Qian and Y.S. Choo

Published by Research Publishing, Singapore.
ISBN: 978-981-11-0745-0; doi:10.3850/978-981-11-0745-0_011-cd

Ajax ONESIDE is another kind of blind bolts, from Ajax Fasteners Company in Australia, which also has five parts: bolt, collapsible washer, shear sleeve, solid washer and nut. Its behavior is very similar to that of traditional high strength bolt and much better than Hollo-bolt (Lee 2010) in the view of pretension. But the bolt may rotate together with the nut during the installation process, which causes inconvenience of construction (Xu 2015).

In order to avoid the defects, the research group of Tongji University developed a novel blind bolt able to apply high preload force, named split-critical blind bolt (SCBB) (Xu 2015). According to the research conclusions, the relative slippage between the connected plates was large because of the enlarged bolt hole on the plate. Wang et.al (2017) presented an experimental research on beam-to-column blind bolted end-plate connections using SCBBs while additional sleeve was adopted. The specimens were designed based on the criteria of strong column to weak beam. However, since the early occurrence of flange local buckling, the beam in the test did not reach its full plastic moment. On the other hand, the concrete slab in the actual beam-to-column joints was not taken into account in the tests.

In this paper, the tests following the previous work by Wang et al. are presented. However, the first difference is the using of compact section beam and reduced section beam (dog-bone section), and the second one is the concrete slab over the reduced section steel beam. The initial stiffness, failure modes, hysteretic behavior and ductility of specimens under cyclic load are studied and discussed.

2 Behavior of Improved SCBB

In order to install the blind bolt outside the tube column, the bolt hole has to be enlarged. This may result in larger slip between column wall and end-plate than that of common high strength bolt, when the external force is greater than the frictional force (Xu 2015). Therefore, an additive sleeve as a component of SCBB is used to infill the gap in bolt hole. The experiments of anti-sliding in slip-critical connection were performed (Jiao 2017). The test results indicated that the existence of additive sleeve could effectively decrease the relative displacement between connected plates, as shown in Figure 1a. In the Figure, the notations of F and F_s refer to the applied load and frictional force, respectively. The sleeve also increased the ultimate shear bearing capacity of bolt for the shear failure of SCBB (Figure 1b). Meanwhile, the behavior of slip-critical connection with improved SCBBs was studied and the research consequence showed that the slip-critical connection could meet the requirements of Chinese code (2017).

3 Experimental Program for beam-column connection with improved SCBB

3.1 *Test specimens*

The purpose of the experiment is to check the elastic stiffness, resistance as well as seismic performance of the beam-column joint with the improved SCBBs. The joint is expected to possess higher strength than plastic moment capacity of connected beams. Three specimens were designed. One with the uniform built-up section beam was used to develop the plastic hinge mechanism of beam, rather than local buckling of beam which was reported by Wang et al. (2017). In order to avoid the possible fracture of weld between beam and end-plate, reduced section beam (RSB) with dog-bone section was adopted for the second specimen. The third specimen designed concrete slab over the beam as that in the actual building structures. On the other hand, the stiffness of joint was enhanced by thickened column wall and concrete filled column, so that the joint was able to be identified as rigid one. The details of all specimens are summarized in Table 1. And the geometric dimensions of reduced beam section are shown in Figure 2. For all specimens, four rows of M24 SCBB were used to connect the end-plate to

column wall and the extended parts of end-plates were reinforced by stiffeners, as shown in Figure 3.

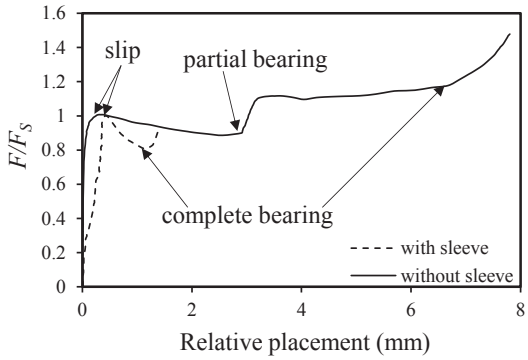

a. The function of additive sleeve

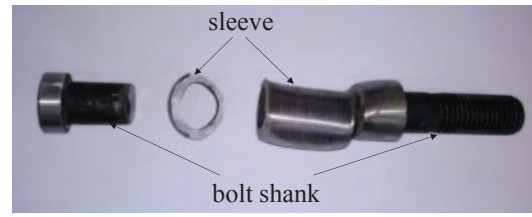

b. Shear failure of SCBB

Figure 1. Test results of slip-critical connection.

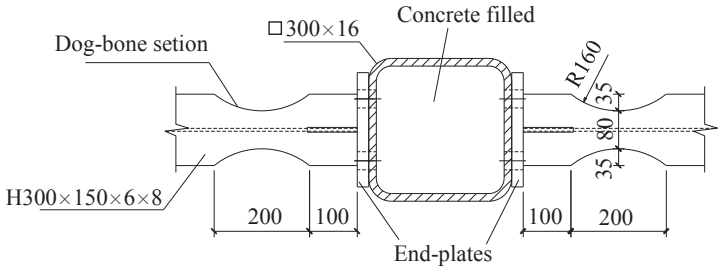

Figure 2. Geometric dimensions of reduced beam section.

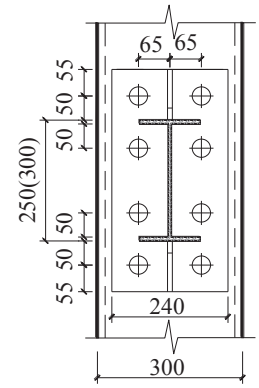

Figure 3. Layout of SCBBs.

Table 1. Summary of test specimens.

Specimen No.	Column (mm)	Beam (mm)	Axial load ratio n	Notes
S1	300×16	250×125×6×8	0.1	Uniform built-up section beam
S2		300×150×6×8		RSB
S3				Concrete slab over RSB

Table 2. Mechanical properties of steel and rebar.

Steel type	f_y (MPa)	f_u (MPa)	Elongation at fracture
Column	413	598	36%
Beam	380	519	34%
End-plate	417	601	39%
Reinforcing steel bar	504	703	39%

The steel used for specimens was Q345 with normal yield stress of 345MPa, and the reinforcing steel bars in the slab were HRB400 with yield stress of 400MPa. The mechanical properties of steel and bar are listed in Table 2. The 150 mm concrete cubes were tested, and the average compressive strength, $f_{c,con}$, was 28.4 MPa.

In order to satisfy the requirements of strong column-weak beam referring to GB 50011 (2016), the plastic moment for CFT-RHS column of $(1\text{-}n)M_{pc}$ should be not less than the enlarged plastic moment ηM_{pb} for steel beam or composite beam. η is a coefficient related to seismic grade for the moment resistant frame. When the ultimate moment resistance M_u of bolted connection is not less than the value of $1.35M_{pb}$ for one beam member, the specimen can meet the design criteria of strong connection-weak component. All the test specimens met the design criteria by calculation according to their nominal size and its nominal strength.

3.2 *Test set-up*

The test set-up is shown in Figure 4 and Figure 5. Spherical hinges were fixed at the top and bottom of the column and hydraulic jack was set at the column top to apply a constant axial compression. The distance of 3615mm between the center of two spherical hinges was taken as the effective length of column. Two hydraulic actuators were positioned at the free ends of beams to conduct cyclic loads. The distance between free ends of beams was 3600mm. A triangular frame was used to connect the column top as the reaction frame. Out-of-plane displacement was constrained by two pairs of lateral bracings with universal ball joints on contact surface.

3.3 *Loading procedure*

Quasi-static cyclic loading procedure was determined on the basis of AISC 341-10 (2010), as shown in Figure 6. In the whole procedure, antisymmetrical loads were applied at the beam free ends by vertical displacement of hydraulic actuators.

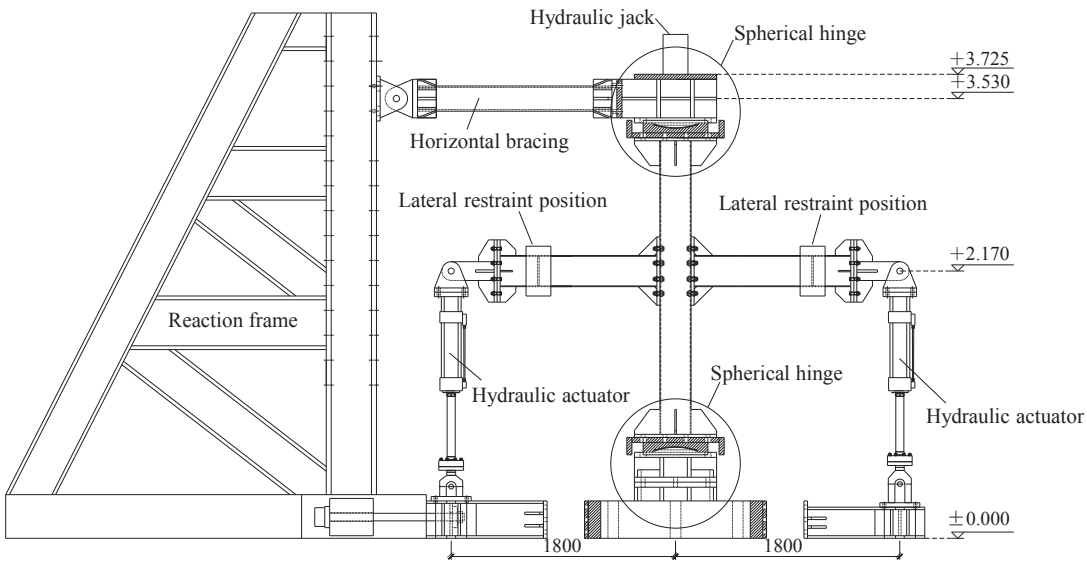

Figure 4. Schematic of test set-up.

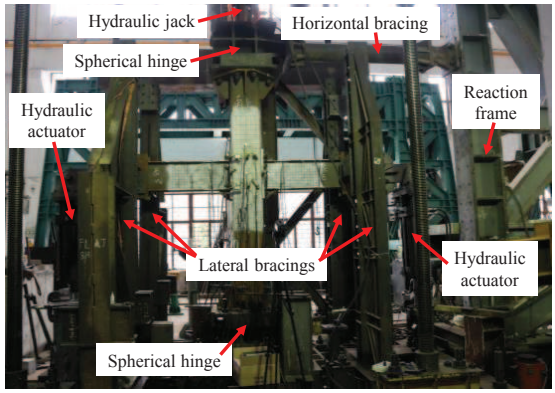

Figure 5. Test set-up on site.

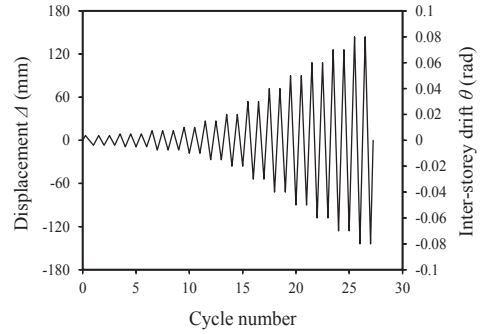

Figure 6. Cyclic loading procedure.

4 Test Results and Discussion

4.1 *Initial stiffness and joint classification*

According to Eurocode 3 (2005), to clarify joint classification should consider the frame features being side sway or not, as well as the ratio of joint initial stiffness S_{ini} to the beam stiffness.

The joint initial stiffness S_{ini} was measured by test. The measured data are listed in Table 3. While, for specimen S3, the notation 'up' and 'down' refers the direction of beam free end displacement. During the test, Linear Variable Displacement Transducers (LVDTs) were used to measure the displacements resulted from the applied loads, including vertical displacements of beam ends (referring to general rotation of specimen), horizontal displacements of the column ends (rigid rotation of specimen) and shear deformation of the panel zones. In order to calculate the joint initial stiffness S_{ini}, the local joint rotation can be obtained by the general rotation of specimen subtracting the sum of elastic deflection of the beam, column and rigid rotation of specimen.

Calculating the beam stiffness should consider the beam span which is not equal to the specimen cantilever length, L_{exp}, or simply doubling it. The equivalent beam span, L, is determined in this study by the following procedure. Firstly the beam end moment, M_G, produced by gravity load, is estimated in the range of 0.3 to 0.5 times of M_e, the beam section edge yielding moment. Then, supposing the beam end moment shall be its fully plastic moment by earthquake action, thus the equivalent beam span, L, can be deduced as shown in Figure 7. Thus we get the beam stiffness so that the classification can be reasonably obtained. The results are listed in Table 3. It shows that the thickened column wall and concrete filled column make the joints belonging to rigid ones.

Table 3. Initial stiffness and joint classification.

Specimen No.	Beam span (mm)		S_{ini} (kN·m/rad)	Classification	
	$M_G = 0.3M_e$	$M_G = 0.5M_e$		$M_G = 0.3M_e$	$M_G = 0.5M_e$
S1	4310	5080	54838	Rigid (sway)	Rigid (sway)
S2	4150	4430	46027	Rigid (no-sway)	Rigid (no-sway)
S3	4010	4240	78188(up) 65529(down)	Rigid (both, no-sway)	Rigid (both, no-sway)

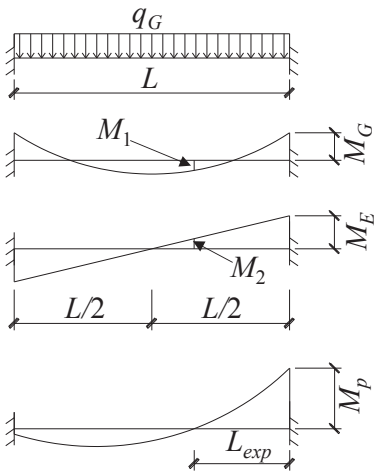

Moment diagram against gravity load:

$$M_G = \frac{q_G L^2}{12} = \alpha M_e \quad (\alpha = 0.3\sim0.5)$$

$$M_1 = \frac{q_G L L_{exp}}{2} - \frac{q_G L_{exp}^2}{2} - M_G$$

Moment diagram against earthquake load:

$$M_E = M_p - M_G$$

$$\frac{L/2 - L_{exp}}{L/2} = \frac{M_2}{M_E}$$

Moment diagram by combined loads:

$$M_1 - M_2 = 0$$

Figure 7. Calculation method of the equivalent beam span.

4.2 *Failure modes*

For specimen S1, the beam developed plastic deformation at first, then flange buckling occurred when subjected to compression and repeated under cyclic moment. After the beam end moment exceeded the plastic moment several times, fracture appeared at the middle of buckling wave (Figure 8a) when the equivalent storey drift θ reached 6%.

For specimen S2, the failure process was similar to S1. However, the weakest section of RSB developed plastic deformation concentrated, and the local buckling was more obviously not only in flange but in web. Lateral-torsional buckling of beam then happened when θ around 4%. The ductile fracture ran through the narrowest flange width (Figure 8b) when θ around 5%.

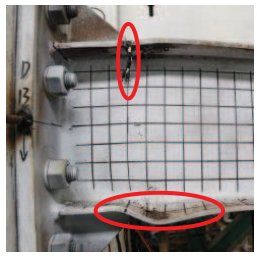

a. Failure mode of S1

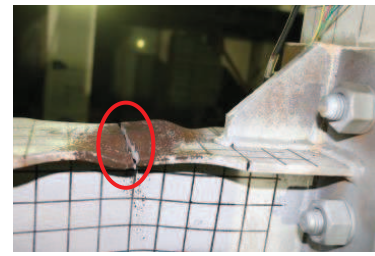

b. Failure mode of S2

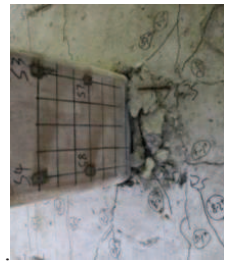

c. Failure mode of S3

Figure 8. Failure modes for three test specimens.

Due to the existence of concrete slab over the beam, the failure mode of specimen S3 was different from specimen S2. The top flange of steel beam was restrained by the concrete slab,

and the neutral axis of the composite section was near the upper flange. Therefore, the plastic deformation of beam concentrated on its bottom flange, so did the local flange buckling deformation (Figure 8c). The part of concrete slab surround the tube column was severely damaged as shown in Figure 8c when the story drift approached 7%.

On the other hand, no joint failure mode was observed in these specimens.

4.3 *Hysteretic behavior and ductility*

Energy was dissipated by plastic deformation of steel beams for specimens S1 and S2 so that the hysteresis curve were sindlel (Figure 9a and 9b). The hysteresis curve of specimen S3 exhibited difference when positive moment or negative moment applied at the joint (Figure 9c) and the plastic moment M_{pb}^{+} and M_{pb}^{-} represent the tension zone of beam section below or above the neutral axis. In addition, no pinch effect was observed in the moment-rotation curves, indicating no slippage occurred on the surface between column wall and end-plate.

The ductility can usually be evaluated in a quantitative manner. Based on the demands in AISC, the drift $\theta_{0.8}$ of specimen should be greater than 0.04rad when the resistance decreases to 80 percent of its ultimate strength. The results of each specimen are listed in Table 4 and exhibit that all the specimens satisfy the ductility requirements in AISC. And the results also demonstrate that the joints with plastic hinge of beam display better ductility than those with inelastic buckling of beam.

5 Conclusions

The improved SCBB by additive sleeve infilling the enlarged bolt holes was used in the extended end-plate connections to CFT-RHS columns. By cyclic loading tests, the main conclusions can be obtained as follows:

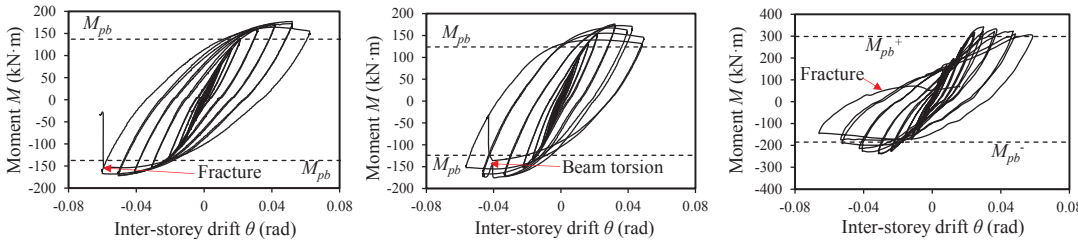

Figure 9. Moment-rotation curves of each specimen.

Table 4. Assessment of ductility.

Specimen No.	$\theta_{0.8}$ (rad)	
	positive direction	negative direction
S1	0.061	0.059
S2	0.049	0.056
S3	0.058	0.055

(i) The initial stiffness of joints can significantly be enhanced by the means of thickened tube wall and concrete filled column, so that they may be satisfied with the rigid joint behavior according to Eurocode 3. The SCBB with additive sleeve could be used in the connections to CFT-RHS columns for moment resistant frames.

(ii) The joint strength can guarantee the connected beam with compact section to develop fully plastic moment.
(iii) The joint adopting improved SCBB can exhibit excellent seismic behaviors, including ductility, energy dissipating ability, without any observed tension relaxing of the SCBB.

References

ANSI/AISC 341-10: *Seismic Provisions for Structural Steel Buildings*, American Institute of Steel Construction, USA, 2010.

Elghazouli A.Y., Malaga-Chuquitaype C., Castro J.M., Orton A.H., Experimental Monotonic and Cyclic Behavior of Blind-bolted Angle Connections, *Eng. Struct.*, 31, 2540-2553, 2009.

EN 1993-1-8: 2005, *Eurocode* 3: *Design of steel structures - Part* 1-8*: Design of joints*, European Committee for Standardization, Brussels, 2005.

GB 50011-2010 (ed. 2016), *Code for Seismic Design of Buildings*, Chinese National Code, China, 2016.

GB 50017-2017, *Standard for Design of Steel Structures*, Chinese National Code, China, 2017.

Jiao W.F., Chen Y.Y., Wang W., Experimental Study on Slip Resistance of the Innovative Single-side Bolt in Friction-type Connection, Proc. of the 15th East Asia-Pacific Conf. on Struct. Eng. and Constr., Xi'an, China, 2017.

Lee J., Goldsworthy H.M., Gad E.F., Blind Bolted T-stub Connections to Unfilled Hollow Section Columns in Low Rise Structures, *J. Constr. Steel Res.*, 66, 981-992, 2010.

Liu Y., Malaga-Chuquitaype C., Elghazouli A.Y., Response and Component Characterization of Semi-rigid Connections to Tubular Columns Under Axial Loads, *Eng. Struct.*, 41, 510-532, 2012.

Loh H.Y., Uy B., Bradford M.A., The Effects of Partial Shear Connection in Composite Flush End Plate Joints Part I-Experimental Study, *J. Constr. Steel Res.*, 62, 378-390, 2006.

Tizani W., Ridley-Ellis D.J., *The Performance of a new Blind-bolt for Moment-Resisting Connections*, Proc. of the 10th Int. Symp. on Tub. Struct., Rotterdam, 2003.

Wang J.F., Han L.H., Uy B., Hysteretic Behavior of Flush End Plate Joints to Concrete-filled Steel Tubular Columns, *J. Constr. Steel Res.*, 65, 1644-1663, 2009.

Wang J.F., Spencer Jr B.F., Experimental and Analytical Behavior of Blind Bolted Moment Connections, *J. Constr. Steel Res.*, 82, 33-47, 2013.

Wang W., Li M.X., Chen Y.Y., Jian X.G., Cyclic Behavior of Endplate Connections to Tubular Columns with Novel Slip-critical Blind Bolts, *Eng. Struct.*, 148, 949-962, 2017.

Wang Z.Y., Tizani W., Wang Q.Y., Strength and Initial Stiffness of A Blind-bolt Connection based on the T-stub Model, *Eng. Struct.*, 32, 2505-2517, 2010.

Xu T., Development of One-side Bolt and Experimental Study on Its Connection Behavior, *Tongji Universiy*, Shanghai, China, 2015.

Xu T., Wang W., Chen Y.Y., A Review on Foreign Research Status of One-side Bolt, *Steel Constr.*, 8(30), 27-33, 2015.